A total synthetic approach to CRISPR/Cas9 genome editing and homology directed repair

Sara E. DiNapoli[1,2 *], Raul Martinez-McFaline[1,2 *], Caitlin K. Gribbin[1,2*], Courtney A. Balgobin[1,2], Isabel Nelson[1,2], Abigail Leonard[1,2], Darya Mailhiot[4], Clara Kao[5], Sean McDonnell[5], Jill L.O. de Jong[5], Yariv Houvras[1,2,3 **]

1. Department of Surgery, Weill Cornell Medical College, New York Presbyterian Hospital, New York, NY, USA
2. Meyer Cancer Center, Weill Cornell Medical College, New York Presbyterian Hospital, New York, NY, USA
3. Department of Medicine, Weill Cornell Medical College, New York Presbyterian Hospital, New York, NY, USA
4. Department of Surgery, Animal Resources Center, University of Chicago, Chicago, IL, USA
5. Department of Pediatrics, University of Chicago, Chicago, IL, USA

* These authors contributed equally to this work.

** Correspondence and requests for materials should be addressed to Y.H. (email: yah9014@med.cornell.edu).

ABSTRACT

CRISPR/Cas9 has become a powerful tool for genome editing in zebrafish that permits the rapid generation of loss of function mutations and the knock-in of specific alleles using DNA templates and homology directed repair (HDR). We directly compared synthetic, chemically modified sgRNAs to *in vitro* transcribed sgRNAs and demonstrate the increased activity of synthetic sgRNAs. We harnessed the efficacy of synthetic sgRNAs to generate large chromosomal deletions over 100kb in size. By developing an *in vivo* genetic assay to measure HDR efficiency, we systematically examined the characteristics of synthetic DNA templates to promote HDR. Utilizing these principles, we successfully performed precise knock-in of fluorophores at multiple genomic loci. Collectively, our studies demonstrate the utility of enhanced synthetic sgRNA activity for a wide range of applications *in vivo* including precise homology directed repair and genome editing.

INTRODUCTION

CRISPR/Cas9 has been utilized for a wide range of experimental applications, and zebrafish has been a key model organism to test and validate strategies for genome editing[1,2]. Repair of CRISPR-generated double-stranded breaks (DSBs) by non-homologous end joining (NHEJ) leads to insertions and deletions (indels) which may result in loss of function of the targeted gene product. By supplying an exogenous DNA template, DSBs are repaired through homology directed repair (HDR), allowing for precision genome editing, including base pair changes and insertion of protein tags. Although HDR has been reported in zebrafish, the efficiency varies widely and has required the construction of vectors to serve as a DNA template[3–7]. While diverse approaches and molecular tools have been reported to improve HDR efficiency in mammalian systems, a comprehensive assessment of strategies for genome editing in zebrafish has not been undertaken.

Recent reports have described an increased efficiency of CRISPR/Cas9 targeting using chemically modified synthetic sgRNAs in human cells[8,9]. We systematically evaluated synthetic sgRNAs and find they dramatically outperform conventional *in vitro* transcribed sgRNAs. Synthetic sgRNAs lead to increased targeting, an expanded range of indels, and allow the generation of large scale deletions in the genome. We developed an assay for HDR in zebrafish utilizing an *mitfa* mutant, b692. This assay allowed us to quantitatively compare multiple strategies for improving HDR efficiency and correlate phenotypic and molecular efficiency. We demonstrate that synthetic reagents, including linear dsDNA templates, can effectively be used to perform precise genomic editing including generation of in-frame gene fusions with fluorophores.

RESULTS

Synthetic sgRNAs outperform laboratory synthesized sgRNAs

In order to directly compare editing efficiencies generated by synthetic sgRNA versus *in vitro* transcribed sgRNA (IVT sgRNA), we targeted tyrosinase (*tyr*), a gene required for melanin synthesis. Wild type zebrafish embryos were microinjected at the one-cell stage with recombinant Cas9 protein (rCas9) complexed with either synthetic sgRNA (IDT, Alt-R®) or with laboratory synthesized IVT sgRNA. Embryos were scored for melanocyte number at 48 hours post-fertilization (hpf) and divided into phenotypic categories representing the degree of gene editing (Figure 1b). We find that the synthetic sgRNA leads to a significantly increased fraction of embryos with fewer melanocytes as compared with IVT sgRNA (Figure 1a). An increasing dose of synthetic sgRNA results in an increase in the fraction of phenotypically edited embryos. Only synthetic sgRNAs were capable of producing large numbers of embryos with high phenotype gene editing. We found comparable differences between synthetic and IVT sgRNAs at a second locus, *slc24a5* (Supplementary Figure 1). In several cases injection of synthetic sgRNAs leads to highly penetrant phenotypes in F_0 larvae that phenocopy established germline mutants[10] (Supplementary Figure 2). In order to

90 characterize the molecular alterations arising in synthetic sgRNA injected embryos, we
91 performed a clonal analysis. We find that 10/10 clones from a synthetic sgRNA injected
92 high-phenotype embryo contain indels, as compared with 7/10 clones from an IVT
93 sgRNA injected high-phenotype embryo. An analysis of indel spectrum and distribution
94 reveals larger deletions in synthetic sgRNA injected embryos (Figure 1c). Taken
95 together, these data indicate that synthetic sgRNAs lead to penetrant phenotypes that
96 are associated with a broad spectrum of gene-specific edits.
97
98 To assess the extent of germline transmission of edited alleles, we applied CRISPR-
99 STAT fluorescence-based genotyping to F_0 founders and progeny[11]. Sperm samples
100 were collected from F_0 founders injected with rCas9 and synthetic sgRNA targeting
101 *slc6a15* at the one-cell stage. Results reveal mutant alleles containing indels as the
102 major peaks, with additional minor peaks corresponding to wildtype and mutant alleles,
103 indicating a high efficiency of CRISPR-induced mutagenesis in the germline (Figure 2a).
104 Five distinct alleles were transmitted to F_1 progeny (Figures 2b-f). The frequencies of
105 observed CRISPR-induced indels in F_1 progeny were similar to those found in the
106 sperm of the F_0 founder (Supplementary Figure 3). These findings are consistent with
107 high levels of somatic mosaicism and confirm that F_0 sperm samples accurately predict
108 the specific mutations transmitted to F_1 progeny. These data demonstrate that CRISPR-
109 induced indels created with synthetic sgRNAs are found in the germline of founders and
110 are efficiently transmitted to F_1 progeny.
111
112 **Synthetic sgRNA pairs produce large chromosomal deletions**
113
114 We assessed whether the enhanced efficiency of synthetic sgRNAs would enable the
115 generation of large chromosomal deletions. We sought to examine the efficiency of
116 synthetic sgRNAs to produce deletions in a region of noncoding DNA (Figure 3a). We
117 designed two sgRNAs situated 453bp apart and co-injected with rCas9. We assayed
118 injected embryos using deletion-specific PCR. We observed the presence of a deleted
119 allele in 5/10 (50%) embryos (Supplementary Figure 4a). Sequencing of an amplicon

120 revealed a deletion of 427 nucleotides (Figure 3B). We co-injected rCas9 with sgRNAs
121 situated 4,286bp apart. By deletion-specific PCR, we identified the presence of a
122 deletion in 7/24 (29%) embryos (Supplementary Figure 4c). Deletions between 4297
123 and 4451 nucleotides were confirmed by Sanger sequencing (Figure 3d and
124 Supplementary Figure 4d). We tested our ability to delete larger regions by co-injecting
125 rCas9 with additional sgRNAs. We observed deletions of 52kb in 3/8 (38%) embryos by
126 PCR and confirmed a deletion of 52, 262 nucleotides by Sanger sequencing
127 (Supplementary Figure 4e,f and Figures 3e). Using sgRNAs spanning the entire non-
128 coding region we generated a deletion of 124KB in 2/23 (9%), which was confirmed by
129 Sanger sequencing (Supplementary Figure 4g,h and Figure 3f). We find that pairs of
130 synthetic sgRNAs are highly efficient in causing large scale deletions in zebrafish, and
131 that the efficiency varies with size (Figure 3a).
132
133 **A genetic assay for homology-directed repair**
134
135 To develop a reliable assay for detecting HDR in zebrafish embryos, we sought to target
136 a locus that could provide phenotypic and molecular evidence of DNA template
137 integration. We initially examined the widely used *mitfa*(w2) mutant, which lacks
138 melanocytes[12]. Unexpectedly, injection of rCas9 complexed with a synthetic sgRNA
139 targeting the mutation site in w2 resulted in restoration of pigmented melanocytes
140 (Supplementary Figure 5). We presume that indels caused by targeting the *mitfa*(w2)
141 mutation site (Q113Stop) restore protein function since this region of the protein is
142 relatively unstructured. We next examined the *mitfa*(b692) which harbors a mutation
143 leading to a Ile215Ser substitution and lacks melanocytes[13]. We find that a synthetic
144 sgRNA targeting the *mitfa*(b692) mutation site does not restore pigmented melanocytes
145 (Supplementary Figure 5). Therefore, we utilized *mitfa*(b692) to examine a broad range
146 of synthetic reagents and approaches to achieve precise HDR.
147
148 We performed an *in vivo* screen to compare the efficiency of HDR across multiple
149 conditions. *mitfa*(b692) embryos were microinjected with rCas9, synthetic sgRNA, and a

150 matrix of synthetic templates designed to restore the wildtype *mitfa* sequence and gene
151 function. Microinjected embryos were scored at 48hpf for phenotypic evidence of
152 melanocytes, indicative of template integration and mitfa function (Figure 4B).
153 Melanocytes were not identified in uninjected embryos or in embryos injected with non-
154 targeting sgRNA (Figure 4b). HDR templates were designed to feature multiple
155 barcoded nucleotides and mutated PAM recognition sequence, enabling unambiguous
156 detection by sequencing and preventing re-cleavage by rCas9 (Figure 4a). Melanocyte
157 positive embryos were subject to allele-specific PCR and Sanger sequencing to confirm
158 precise HDR (Figures 4c and d).
159
160 We found that a 951bp, double-stranded linear DNA template with an asymmetric
161 sgRNA site located at the 3' end leads to a reproducible 9% rate of phenotypic rescue in
162 *mitfa*(b692) embryos (Figure 4a and e). We examined DNA templates that differ in
163 length, single vs. double stranded DNA, linear vs. circular templates, and the symmetry
164 of the sgRNA position within the template (Figure 4e). We find that both longer (2kb)
165 and shorter (318bp, 76bp) DNA templates led to a decrease in HDR efficiency.
166 Asymmetric positioning of sgRNA sites led to higher efficiency than symmetric
167 positioning. Our data indicates that HDR efficiency is maximal with dsDNA templates
168 and is sensitive to template length and symmetry of the sgRNA site.
169
170 Using the b692 assay we examined multiple reagents and conditions reported to
171 improve HDR efficiency in other model systems (Figure 4e and Supplementary Figure
172 6). The addition of a second sgRNA site to the optimal 951bp template reduced HDR
173 efficiency to < 1%. We cloned the 951bp template into a TopoTA plasmid vector and
174 microinjected a circular plasmid into zebrafish. This plasmid-based template also failed
175 to lead to measurable HDR in b692 embryos. In light of prior studies reporting increased
176 HDR efficiency with the use of catalytically-mutated Cas9 (nickase Cas9)[14], we altered
177 the 951bp DNA template to allow us to test this approach. Microinjection of paired
178 sgRNAs and recombinant nickase Cas9 failed to lead to measurable HDR in b692
179 embryos. Microinjection of ssDNA templates and small molecule poly (ADP-ribose)

180 polymerase (PARP) inhibitors also failed to lead to measurable HDR efficiency. A
181 complete summary of the tested reagents and phenotypic editing efficiency is
182 summarized (Supplementary Figure 6).
183
184 **Melanocyte restoration in b692 assay correlates with molecular efficiency**
185
186 Using the b692 assay we sought to measure the molecular efficiency of genome editing
187 and correlate DNA template integration with melanocyte number. To this end, we
188 performed single-cell injections in a large cohort of b692 embryos using the optimized
189 reagents described: rCas9, synthetic b692 sgRNA, and 951bp linear dsDNA template.
190 Embryos were scored for the presence of melanocytes at 48hpf and binned by
191 phenotype into four categories: high, medium, low, and no-editing. Uninjected embryos
192 were included as a negative control. Genomic DNA was extracted from pools of five
193 embryos in each category and exon 7 was amplified by PCR. Amplicons from each
194 group were subjected to next-generation sequencing. We find that that the efficiency of
195 genome editing as determined by next-generation sequencing correlates with
196 phenotype in b692 edited embryos. In high rescued embryos we find that 17% of reads
197 (106428 edited/641281 total) harbor an edited codon restoring Ser215 to Ile, consistent
198 with template integration. Analysis of aligned reads at exon 7 reveals the uniform
199 presence of barcoded nucleotides from the HDR template across the sgRNA target site.
200 Phenotypic rescue in medium and low categories revealed molecular efficiency of
201 approximately 3% (14810/575344 and 17566/622068 reads, respectively). Injected
202 embryos with no phenotypic evidence of HDR had molecular efficiency of <0.3%.
203 Alignment of reads demonstrates a mutually exclusive pattern of either HDR and
204 template integration or indels at the sgRNA site (Figure 5a), consistent with a highly
205 efficient dsDNA cleavage. We analyzed the molecular efficiency across all phenotypes
206 and plotted the fraction of reads harboring barcoded nucleotides from the HDR template
207 (Figure 5b-e). These data confirm the sensitivity of the b692 assay to read out the
208 molecular efficiency of HDR *in vivo*.
209

210 **Genome editing using synthetic reagents leads to efficient fluorophore knock-in**

211

212 To determine the feasibility of using synthetic reagents to knock-in a fluorophore with
213 HDR, we targeted *tyrp1b*, a melanocyte-specific gene. Using albino embryos
214 (pigmentless due to a null mutation in *slc45a2*) we performed microinjection of rCas9
215 with a synthetic sgRNA and a synthetic linear dsDNA template designed to knock EGFP
216 in frame with the terminal *tyrp1b* exon (Figure 6a). We identified 7/153 (5%) embryos
217 with EGFP-positive melanocytes at 48hpf (Figure 6b). Confocal imaging revealed the
218 presence of an EGFP-positive melanocyte with characteristic stellate morphology
219 (Figure 6d). Allele-specific PCR was performed from injected embryos with EGFP-
220 positive melanocytes (Figure 6e). Sanger sequencing revealed the presence of multiple
221 barcoded nucleotides encoded by the HDR template, consistent with precise integration
222 (Figures 6c).

223

224 To determine the generalizability of this approach across multiple loci, we targeted
225 *h3f3a*, one of several genes encoding histone H3.3. We designed a linear dsDNA
226 template to knock EGFP in frame with *h3f3a*, creating a C-terminal fusion (Figure 6f).
227 We microinjected rCas9 with a synthetic sgRNA targeting *h3f3a* and synthetic dsDNA
228 template into wild type embryos. We identified 12/152 (8%) embryos with EGFP-positive
229 cells at 48hpf (Figure 4g). Confocal imaging revealed the presence of nuclear EGFP-
230 positive cells characteristic of chromatin (Figure 6i). Allele-specific PCR and Sanger
231 sequencing performed on EGFP positive embryos revealed precise template integration
232 (Figure 6h and j). Taken together these data demonstrate the ability of synthetic
233 sgRNAs and dsDNA templates to knock-in allele-specific fluorophores at several
234 genomic loci.

235

236 **DISCUSSION**

237

238 Here we describe the development and application of genome editing in zebrafish using
239 synthetic reagents. We show that synthetic sgRNAs combined with recombinant Cas9

240 protein leads to highly efficient indels as compared to conventional laboratory
241 synthesized sgRNAs. We speculate that improved efficiency of commercial sgRNAs
242 results from both the chemical modifications that protect sgRNAs from degradation and
243 the increased fidelity of solid phase chemical synthesis. Our studies demonstrate
244 germline transmission of synthetic sgRNA induced mutations to F_1 animals following
245 detection of mutant alleles in the sperm of F_0 animals. While previous reports have
246 generated smaller deletions in zebrafish[15], we demonstrate that synthetic sgRNAs can
247 produce deletions up to 124kb. Our approach to knock-in synthetic linear dsDNA
248 templates has broad applications for studying specific cell populations in development,
249 for engineering disease causing mutations, and for following clones of cells in mosaic F_0
250 animals.
251
252 In order to understand the parameters critical for homology-directed repair we
253 developed a genetic assay using *mitfa*(b692) mutant zebrafish. The b692 assay is
254 highly sensitive and allowed us to systematically examine multiple variables associated
255 with HDR efficiency. We find that template length, strandedness, and sgRNA site
256 symmetry appear to be the most critical variables in our model. A key aspect of our
257 study is the empirical test of multiple conditions reported to improve HDR in other
258 contexts, using tools such as single-stranded short DNA templates, PARP inhibitors,
259 multiple sgRNA sites, catalytically mutated rCas9[14,16,17]. In our hands these approaches
260 do not translate to efficient HDR in zebrafish, suggesting that requirements for HDR
261 may be species specific.
262
263 A total synthetic approach has the unique advantage that reagents can be designed *in*
264 *silico* and commercially manufactured in a short time frame. Design and precision
265 editing with a synthetic dsDNA template can generally be accomplished within 2 weeks.
266 The use of synthetic reagents creates unique possibilities for future studies. The use of
267 sgRNAs produced by commercial solid phase synthesis raises the possibility of
268 incorporating degeneracy in the sgRNA sequence to permit a single sgRNA to target
269 multiple related genes. The synthesis of linear dsDNA templates may allow

270 investigators to rapidly test sequence requirements for HDR. As new recombinant Cas9
271 proteins become available the ability to perform base editing and other enzyme
272 modifications may be possible. Finally, the b692 assay may be used as a screening
273 platform to identify chemical and genetic modifiers of HDR efficiency.
274
275 The use of CRISPR/Cas9 to generate loss of function mutations in zebrafish and other
276 model organisms makes it a uniquely valuable resource for forward genetics. To our
277 knowledge, this is the first head-to-head study investigating the effects of synthetic
278 versus *in vitro* transcribed guide RNAs and to perform a comprehensive optimization of
279 HDR efficiency in zebrafish. Our studies offer insight into the relative efficiency of HDR
280 and provide investigators with a highly efficient workflow for generating edited alleles,
281 and precise gene knock-ins. We find a single synthetic sgRNA is highly efficient in
282 generating on-target loss of function indels in a majority of tested genes. Our approach
283 to genome editing should allow investigators to pursue a broad range of *in vivo*
284 applications including high efficiency mutant generation, deletion of large genomic
285 regions to study regulatory DNA, and fluorophore and epitope tag knock-in for functional
286 studies. Future improvements in HDR efficiency may occur with new variations in Cas9
287 protein and chemical or genetic tools to further enhance the efficiency of homology
288 directed repair and integration of donor DNA templates.
289
290 **MATERIALS AND METHODS**
291
292 sgRNA sequence design
293 sgRNAs were designed using the design tool sgRNA Scorer 1.0 and 2.0[18,19]
294 GuideScan[20], or CRISPRz[21]. Using GuideScan we selected sgRNAs with zero
295 computed off-targets with a maximum of 3 base mismatches.
296
297 Preparation of *in vitro* transcribed sgRNAs
298 DNA templates for IVT were synthesized as double-stranded gBlock Gene Fragments
299 (Integrated DNA Technologies) containing a T7 binding site with additional 3' G (5'-

300 TAATACGACTCACTATAGG), 20bp target site without PAM site, and 80bp tracrRNA
301 site (5'-
302 GTTTTAGAGCTAGAAATAGCAAGTTAAAATAAGGCTAGTCCGTTATCAACTTGAAAA
303 AGTGGCACCGAGTCGGTGCTTTT-3').
304
305 50ng of sgRNA gBlock (10ng/uL) was *in vitro* transcribed using a SureGuide gRNA
306 Synthesis Kits (Agilent, 5190-7718) in a 25uL reaction and incubated at 37ºC for 3-4
307 hours. Following DNAse digestion sgRNAs were column-purified using standard kit
308 instructions and eluted in H_2O. Concentration was determined using a Nanodrop
309 spectrophotometer and 200ng of the sgRNA was run on an agarose gel for quality
310 control.
311
312 Synthetic sgRNA preparation
313 sgRNA sequences were ordered from Integrated DNA Technologies (IDT) as Alt-R®
314 CRISPR-Cas9 crRNAs. The common tracrRNA was purchased from IDT. The crRNA
315 and tracrRNA were resuspended to 100uM in nuclease-free duplex buffer (IDT)
316 according to manufacturer specifications. Equimolar amounts of crRNA and tracrRNA
317 were heteroduplexed by heating solution to 95ºC for 5 min and then cooled to room
318 temperature for 5-10 min. Dilution of sgRNA complex to a working concentration was
319 done using Nuclease-free Duplex Buffer and stored in -80ºC as single-use aliquots.
320
321 HDR template design
322 HDR templates were ordered as gBlock Gene Fragments (IDT). Synthesized gBlocks
323 were resuspended in nuclease-free water to a concentration of 50ng/uL and stored at -
324 20ºC.
325
326 Microinjection
327 For global editing with a single sgRNA, 250pg sgRNA and 500pg rCas9 were injected
328 into the yolk of one-cell stage embryos. To generate deletions, 250pg sgRNA 1, 250pg
329 sgRNA 2 and 500pg rCas9 were injected into the yolk of one-cell stage embryos. For

330 HDR injections, 250pg sgRNA, 500pg rCas9 and 37.5pg HDR template were injected
331 into the cell one-cell stage embryos.
332
333 gDNA isolation
334 Individual embryos (24-48hpf) were incubated in 150 µl of DirectPCR Lysis Reagent
335 (Viagen, 102-T) containing 20 µg/ml Proteinase K (Qiagen, 158920) at 55°C for 60 min
336 followed by 45 min at 85°C. gDNA was stored at 4°C.
337
338 CRISPR-STAT protocol
339 Sperm samples from potential founders were collected with 10 uL capillary tubes as
340 previously described, and then followed the HOTShot method with 25 uL alkaline lysis
341 buffer to prepare DNA templates[22-23]. Tail clips were prepared similarly. The CRISPR-
342 STAT protocol was used to perform fluorescence-based genotyping[11]. Primers
343 sequences used for the CRISPR-STAT assay were *slc6a15* FOR,
344 tgtaaaacgacggccagtGGCCACGACCTACTACTGGTAT, which includes (lowercase)
345 M13 tag for binding to a fluorescent-labeled M13 primer; and *slc6a15* REV,
346 gtgtcttTATAGATGCTGCGTCACGTTTC, which include the (lowercase) 'PIG tail' tag
347 that helps ensure uniform product size, via Taq adenylation[24]. Relative amounts of each
348 uniquely-sized PCR product (>100 bp, and >100 peak height) were calculated with area
349 under the curve measurements using Applied Biosystems Peak Scanner software.
350
351 Assessment of CRISPR/Cas9 efficiency
352 1uL of genomic DNA was PCR-amplified using specified primers (Supplementary Figure
353 7). 8 uL of PCR product was mixed with 1.6uL NEB Buffer 2 and 6.4uL of water and
354 was incubated at 95ºC for 5 minutes followed by cooling from 95ºC-85ºC at -
355 2°C/second and 85-25°C at -0.1°C/second. 0.4uL NEB Buffer 2, 3.4uL water and 2U of
356 T7EI endonuclease (New England BioLabs, M0302) were added to hybridized products
357 and were incubated for 1 hour at 37ºC. The 20uL reaction was run on a 2% agarose
358 gel.
359

360 For clonal analysis, the PCR product was cloned into pCRII-TOPO (Invitrogen,
361 K460001) as per the manufacturer's instructions and Sanger sequenced (Genewiz).
362 Sequences were compared to reference genome and non-targeting controls to identify
363 indels using CrispRVariants[25] and MacVector (Version 15.5).
364
365 Assessment of deletions
366 gDNA was PCR amplified using primers that flanked the deletion sgRNAs. PCR
367 products were purified (Qiagen, 28104) and Sanger sequenced. Sequences were
368 compared to the reference genome using MacVector.
369
370 Imaging
371 Micrographs of whole embryos and larval animals were taken with a Zeiss Discovery V8
372 stereomicroscope (Zeiss, Oberkochen, Germany) equipped with epifluorescence and
373 appropriate filters. Live imaging of fluorescent larvae was acquired with a Zeiss LSM800
374 laser scanning confocal microscope (Zeiss). For melanocyte counting, 48hpf embryos
375 were visualized under the stereoscope and binned into 4 categories (WT, 100+, 51-100,
376 0-50 melanocytes). Scientists were blinded to the conditions when binning embryos.
377
378 Next-generation sequencing
379 50ng of PCR amplicon DNA was converted into blunt ends using T4 DNA polymerase
380 and *E. coli* DNA polymerase I Klenow fragment. Libraries were prepared using the
381 Kapa_LTP_Library Preparation Kit (Roche, Basel, Switzerland). Multiple indexing
382 adapters are ligated to the ends of the DNA fragments. Ligation reaction products were
383 purified by AMPure XP beads (NEB) to remove all unligated adapters and quantified
384 using Qubit (Thermo Fisher Scientific) and Bioanalyzer DNA chip (Agilent). Indexed
385 sample libraries were normalized and pooled and were sequenced using the Illumina
386 HiSeq4000 sequencer at 2x50 cycles single reads. Reads were aligned to the zebrafish
387 genome (GRCz10) using the Ensembl transcriptome[26]. Results were viewed using
388 Integrative Genome Browser (IGV)[27,28].
389

390 Fish lines and maintenance

391 Zebrafish strains were maintained according to established guidelines[29].Wild-type
392 animals were from the AB background. Experiments were performed in strict
393 accordance with the recommendations in the Guide for the Care and Use of Laboratory
394 Animals of the National Institutes of Health. All of the animals were handled according
395 to approved institutional animal care and use committee (IACUC) protocols of Weill
396 Cornell Medical College.

397

398 Acknowledgements

399 We are grateful to members of the Houvras laboratory for critical discussion and
400 manuscript review. We thank the Weill Cornell Genomics Resources Core Facility for
401 next generation sequencing. This work was supported by the Department of Surgery,
402 Weill Cornell Medical College (YH); National Institutes of Health/National Cancer
403 Institute pre-doctoral fellowship F31CA192813 (SED); National Institutes of
404 Health/National Cancer Institute pre-doctoral fellowship F31CA213997 (RM); the
405 Medical Scientist Training Program of General Medical Sciences of the NIH
406 (T32GM007739) to the Weill Cornell/Rockefeller/Sloan-Kettering Tri-Institutional MD-
407 PhD Program (RM); the Clinical and Translational Science Center at Weill Cornell
408 Medical College TL1-TR0002386-01 (CKG).

409

410 Author Contributions

411 Y.H. conceived and led this work. S.D., R.M., and C.G. designed the genetic assays,
412 performed experiments and conducted data analyses related to genome editing. I.N.,
413 C.B., and A.L. provided technical assistance and performed data analysis. D.M., C.K.,
414 S.M., and J.J. implemented and interpreted the entirety of the CRISPR-STAT
415 protocol. S.D., C.G., and Y.H. wrote the paper.

416 Competing Financial Interests
417 The authors declare no competing financial interests.

418

419 REFERENCES

420 1. Jao, L.-E., Wente, S. R. & Chen, W. Efficient multiplex biallelic zebrafish genome

421 editing using a CRISPR nuclease system. *Proc. Natl. Acad. Sci. U. S. A.* **110,**
422 13904–9 (2013).
423 2. Shah, A. N., Davey, C. F., Whitebirch, A. C., Miller, A. C. & Moens, C. B. Rapid
424 reverse genetic screening using CRISPR in zebrafish. *Nat. Methods* **12,** 535–540
425 (2015).
426 3. Auer, T. O., Duroure, K., Cian, A. De, Concordet, J. & Bene, F. Del. Highly
427 efficient CRISPR / Cas9-mediated knock-in in zebrafish by homology-independent
428 DNA repair. *Genome Res.* **24,** 142–153 (2014).
429 4. Irion, U., Krauss, J. & Nusslein-Volhard, C. Precise and efficient genome editing
430 in zebrafish using the CRISPR/Cas9 system. *Development* 4827–4830 (2014).
431 doi:10.1242/dev.115584
432 5. Hoshijima, K., Jurynec, M. J. & Grunwald, D. J. Precise Editing of the Zebrafish
433 Genome Made Simple and Efficient. *Dev. Cell* **36,** 654–667 (2016).
434 6. Hwang, W. Y. *et al.* Heritable and Precise Zebrafish Genome Editing Using a
435 CRISPR-Cas System. *PLoS One* **8,** 1–9 (2013).
436 7. Kimura, Y., Hisano, Y., Kawahara, A. & Higashijima, S. I. Efficient generation of
437 knock-in transgenic zebrafish carrying reporter/driver genes by CRISPR/Cas9-
438 mediated genome engineering. *Sci. Rep.* **4,** 1–7 (2014).
439 8. Hendel, A. *et al.* Chemically modified guide RNAs enhance CRISPR-Cas genome
440 editing in human primary cells. *Nat. Biotechnol.* **33,** 985–989 (2015).
441 9. Rahdar, M. *et al.* Synthetic CRISPR RNA-Cas9-guided genome editing in human
442 cells. *Proc. Natl. Acad. Sci.* **112,** E7110-7117 (2015).
443 10. Sheets, L., Ransom, D. G., Mellgren, E. M., Johnson, S. L. & Schnapp, B. J.
444 Zebrafish Melanophilin Facilitates Melanosome Dispersion by Regulating Dynein.
445 *Curr. Biol.* **17,** 1721–1734 (2007).
446 11. Carrington, B., Varshney, G. K., Burgess, S. M. & Sood, R. CRISPR-STAT: An
447 easy and reliable PCR-based method to evaluate target-specific sgRNA activity.
448 *Nucleic Acids Res.* **43,** 1–8 (2015).
449 12. Lister, J., Robertson, C., Lepage, T., Johnson, S. & Raible, D. Nacre Encodes a
450 Zebrafish Microphthalmia-Related Protein That Regulates Neural-Crest-Derived
451 Pigment Cell Fate. *Development* **126,** 3757–3767 (1999).
452 13. Lister, J. A., Close, J. & Raible, D. W. Duplicate mitf genes in zebrafish:
453 Complementary expression and conservation of melanogenic potential. *Dev. Biol.*
454 **237,** 333–344 (2001).
455 14. Richardson, C. D., Ray, G. J., DeWitt, M. A., Curie, G. L. & Corn, J. E. Enhancing
456 homology-directed genome editing by catalytically active and inactive CRISPR-
457 Cas9 using asymmetric donor DNA. *Nat. Biotechnol.* **34,** 339–344 (2016).
458 15. Varshney, G. K. *et al.* High-throughput gene targeting and phenotyping in
459 zebrafish using CRISPR / Cas9. *Genome Res.* **25,** 1–13 (2015).
460 16. Quadros, R. M. *et al.* Easi-CRISPR: A robust method for one-step generation of
461 mice carrying conditional and insertion alleles using long ssDNA donors and
462 CRISPR ribonucleoproteins. *Genome Biol.* **18,** 1–15 (2017).
463 17. Anantha, R. W. *et al.* Functional and mutational landscapes of BRCA1 for
464 homology-directed repair and therapy resistance. *Elife* **6,** 1–21 (2017).

18. Chari, R., Mali, P., Moosburner, M. & Church, G. M. Unraveling CRISPR-Cas9 genome engineering parameters via a library-on-library approach. *Nat. Methods* **12,** 1–7 (2015).
19. Chari, R., Yeo, N. C., Chavez, A. & Church, G. M. SgRNA Scorer 2.0: A Species-Independent Model to Predict CRISPR/Cas9 Activity. *ACS Synth. Biol.* **6,** 902–904 (2017).
20. Perez, A. R. *et al.* GuideScan software for improved single and paired CRISPR guide RNA design. *Nat. Biotechnol.* **35,** 347–349 (2017).
21. Varshney, G. K. *et al.* CRISPRz: A database of zebrafish validated sgRNAs. *Nucleic Acids Res.* **44,** D822–D826 (2016).
22. Draper, B. W. & Moens, C. B. A High-Throughput Method For Zebrafish Sperm Cryopreservation and In Vitro Fertilization. *J. Vis. Exp.* 1–5 (2009). doi:10.3791/1395
23. Meeker, N. D., Hutchinson, S. A., Ho, L. & Trede, N. S. Method for isolation of PCR-ready genomic DNA from zebrafish tissues. *Biotechniques* **43,** 610–614 (2007).
24. Brownstein, M. J., Carpten, J. D. & Smith, J. R. Modulation of non-templated nucleotide addition by Taq DNA polymerase: Primer modifications that facilitate genotyping. *Biotechniques* **20,** 1004–1010 (1996).
25. Lindsay, H. *et al.* CrispRVariants charts the mutation spectrum of genome engineering experiments. *Nat. Biotechnol.* **34,** 701–702 (2016).
26. Howe, K. *et al.* The zebrafish reference genome sequence and its relationship to the human genome. *Nature* **496,** 498–503 (2013).
27. Thorvaldsdóttir, H., Robinson, J. T. & Mesirov, J. P. Integrative Genomics Viewer (IGV): High-performance genomics data visualization and exploration. *Brief. Bioinform.* **14,** 178–192 (2013).
28. Robinson, J. T. *et al.* Integrative Genomics Viewer. *Nat. Biotechnol.* **29,** 24–26 (2011).
29. Westerfield M. 2007. The Zebrafish Book a Guide for the Laboratory Use of Zebrafish (Danio Rerio). 5th Edition. Eugene: University of Oregon Press.

509
510
511
512
513
514 **Figure 1 Synthetic sgRNAs outperform laboratory synthesized *in vitro* transcribed**
515 **sgRNAs. a**, Dose-response comparison of editing in embryos injected with rCas9 and
516 either an *in vitro* synthesized or synthetic sgRNA targeting *tyr*. Embryos were scored for
517 melanocyte dropout at 48hpf and binned into 4 categories. The percentage of embryos
518 in each condition is plotted. At the 1000pg sgRNA/2000pg rCas9 dose, there is a
519 statistically significant increase in the editing observed with the synthetic sgRNA
520 (p=<0.001, Chi-square). **b**, Light microscopic images of representative embryos in each
521 category. **c**, Distribution of wild type clones, small indels (<5bp), and large indels (>5bp)
522 in embryos injected with synthetic or *in vitro* transcribed sgRNAs. **d**, CrisprVariants
523 (Lindsay et al., 2016) plot of indels in clones isolated from embryos injected with either
524 synthetic or *in vitro* transcribed sgRNAs. 10/10 clones isolated from individual embryos
525 injected with synthetic from sgRNAs contained indels and 7/10 clones isolated from
526 embryos injected with IVT sgRNAs contained indels.
527
528 **Figure 2 Germline transmission of edited alleles is achieved using synthetic**
529 **sgRNAs. a**, Sperm samples were collected from a CRISPR-injected potential F_0
530 founder and assayed using CRISPR-STAT fluorescence-based genotyping. **b-f**,
531 CRISPR-STAT results for tail clips from representative F_1 progeny, each carrying one of
532 the distinct alleles with specific insertions and deletions (del3, del4, del7, del11), as well
533 as the wild type (WT) allele, transmitted from the F0 founder. The number of F1
534 offspring identified with each genotype is identified in the bottom right of each panel.
535 Relative fluorescence levels (y-axis) are shown against fragment size in base pairs (x-
536 axis) for each genotyping assay. PCR products consistent with predicted wild type
537 amplicon size are indicated by red asterisks.
538
539 **Figure 3 Synthetic sgRNA pairs produce large chromosomal deletions. a**,
540 Schematic of a 126kb non-coding region targeted for genomic deletions. Guide
541 locations are marked in purple, and primers used for PCR are displayed as orange
542 arrows. Guide pairs were co-injected into 1 cell stage embryos. **b**, Deletion-specific
543 PCR was performed to confirm the presence of a deletion in individual F_0 injected
544 embryos. The predicted deletion size for each pair and frequency of deletions is shown.
545 **c-f**, PCR amplicons from individual embryos were subjected to Sanger sequencing and
546 analysis of deletions. The observed deletion size is displayed.
547
548 **Figure 4 A genetic assay for optimizing homology-directed repair using synthetic**
549 **reagents. a**, Schematic depicting *mitfa* gene structure and location of the mutation in
550 exon 7 in b692 mutants. Guide locations are marked in purple, and primers used for
551 PCR are displayed as orange arrows. A linear 951bp dsDNA template encodes a wild-
552 type Ile codon at position 215 and several other nucleotide changes for template

553 identification after sequencing. **b**, *mitfa*(b692) embryos uninjected (top), injected with
554 rCas9, 951bp DNA template, and non-targeting sgRNA (middle) or *mitfa* sgRNA
555 (bottom). All embryos shown at 48hpf. **c**, Allele-specific PCR was performed on rescued
556 embryos after microinjection with 951bp template compared with uninjected embryos. **d**,
557 Sanger sequencing results of allele-specific PCR products from a single phenotypically
558 rescued embryo. **e**, Chart depicting attributes of DNA template (left), a description of the
559 template (middle) and observed rate of rescue (right).
560
561 **Figure 5 Quantitative assessment of genome editing efficiency by next-generation**
562 **sequencing. a**, Alignment of next generation sequencing reads from b692 genome
563 edited embryos from the high rescue phenotype. Exon 7 of *mitfa* is displayed. The
564 sgRNA sequence is highlighted in yellow. b692 mutants have a T>G mutation leading to
565 an isoleucine to serine substitution at codon 215(*). The 951bp dsDNA template
566 restores the wild-type isoleucine codon (ATC) and encodes nine additional barcoded
567 nucleotides as indicated. Indels in sequencing reads are represented as gapped regions
568 in black. **b-e**, The fraction of reads at each barcoded nucleotide in the HDR template is
569 plotted for each phenotype category.
570
571
572 **Figure 6 Genome editing leads to precise fluorophore knock-in. a**, Schematic
573 depicting *tyrp1b* locus. A linear, dsDNA template designed to lead to an in-frame EGFP
574 knock-in is shown. **b**, albino(b4) embryo injected with rCas9, *tyrp1b* synthetic sgRNA
575 and dsDNA template is photographed with light (top panel) or fluorescence (bottom
576 panel) microscopy at 48hpf. **c**, Sanger sequencing from allele-specific PCR to detect
577 template integration. The sequence was aligned to reference (top). Barcoded
578 nucleotides at the sgRNA binding site consistent with template integration were
579 identified. A representative chromatogram is shown. **d**, Confocal imaging reveals the
580 presence of stellate EGFP-positive melanocytes. **e**, Allele-specific PCR was performed
581 on uninjected or HDR edited/GFP+ embryos at 48hpf. Only HDR edited/EGFP positive
582 embryos had a PCR amplicon. **f**, Schematic depicting *h3f3a* locus. A linear, dsDNA
583 template designed to lead to an in-frame EGFP knock-in is shown. **g**, Wild type embryo
584 injected with rCas9, *h3f3a* sgRNA and dsDNA template is photographed with light (top
585 panel) or fluorescence (bottom panel) microscopy (48hpf). **h**, Sanger sequencing was
586 performed from allele-specific PCR to detect template integration. The sequence was
587 aligned to reference (top). Barcoded nucleotides at the sgRNA binding site, consistent
588 with template integration were identified. A representative chromatogram is shown. **i**,
589 Confocal imaging reveals the presence of a EGFP-positive nuclei. **j**, Allele-specific PCR
590 was performed on uninjected or HDR edited/GFP+ embryos at 48hpf. Only HDR
591 edited/EGFP positive embryos had a PCR amplicon.
592
593 **Supplementary Figure 1 Synthetic sgRNAs outperform *in vitro* synthesized**
594 **sgRNA in targeting *slc25a2*. a,** Comparison of Alt-R® synthetic sgRNA preparation
595 and *in vitro* synthesis of sgRNAs. Left, Alt-R® synthetic sgRNAs are prepared by
596 duplexing a gene specific crRNA with a common tracrRNA. Right, IVT sgRNAs are

transcribed from a DNA template using RNA polymerase and purified. Both sgRNAs are used with rCas9 and microinjected into embryos at the one-cell stage. **b,** Light microscopic images of representative embryos in each category. **c,** Dose-response comparison of editing in embryos injected with rCas9 and either an *in vitro* synthesized or synthetic sgRNA targeting *slc25a2*. Embryos were scored for melanocyte dropout at 48hpf and binned into 4 categories. The percentage of embryos in each condition is plotted.

Supplementary Figure 2 Synthetic sgRNAs produce highly penetrant phenotypes in F_0 injected animals. Wild-type (AB) embryos were injected with rCas9 and synthetic sgRNA targeting *mlpha*. Uninjected larval animals (top) have normal stripe pattern. Juvenille zebrafish (7 weeks post fertilization) injected with rCas9 and a synthetic sgRNA targeting *mlpha* show reduced pigmentation and phenocopies an established mutant.

Supplementary Figure 3 Indels in F_0 sperm predict alleles transmitted to the germline. Percentages shown are calculated as area under the curve for each peak in the indicated tissue from the F_0 founder. The frequencies of each mutation in the F_1 progeny were calculated from a total of 17 siblings from a cross between the F_0 male parent and a WT female.

Supplementary Figure 4 Detection and verification of chromosomal deletions. a,c,e,g, Deletion-specific PCR was performed to detect deletions from individual embryos injected with rCas9 and the indicated sgRNAs. In **(a)**, the top band is the wild-type allele and the lower band is indicative of a deletion. **b,d,f,h,** Sanger sequencing of PCR products reveals the specific deletions resulting from injection of sgRNA pairs.

Supplementary Figure 5 Comparison of melanocyte phenotypes in mitfa mutants for after targeting mitfa using CRISPR/Cas9. a, *mitfa*(w2) embryos were injected with rCas9 and a specific sgRNA near the mutation site. Ten representative embryos at 24hpf are shown. Melanocyte rescue occurs in a significant fraction of embryos. **b,** CrispRVariants plot from *mitfa*(w2) embryos injected with rCas9 and nacre gRNA. A majority of embryos harbor indels. **c,** mitfa(b692) embryos were injected with rCas9 and a synthetic sgRNA near the b692 mutation site (b692 sgRNA). Uninjected wild-type (AB) embryos (top, left) have pigmented melanocytes at 48hpf. Wild-type embryos injected with rCas9 and b692 sgRNA (bottom, left) have a highly penetrant loss of melanocytes. Uninjected *mitfa*(b692) embryos (top, right) lack pigmentation because of the b692 mutation. *mitfa*(b692) embryos injected with rCas9 and the b692 sgRNA (bottom, right) have no evidence of melanocyte rescue.

Supplementary Figure 6 Strategies employed for optimizing homology-directed repair at *mitfa*. Schematic depicts several different DNA templates employed for HDR in vivo. Mutated sgRNA binding sites are indicated by vertical purple lines and overlapping blue lines indicate shared genomic sequence. Descriptions of each template along with any special considerations are noted in the middle column.

641 Efficiencies of HDR, as measured phenotypically by presence or absence of
642 melanocytes in injected *mitfa*(b692) zebrafish, are noted in the right column.
643
644 **Supplementary Figure 7 sgRNA and primer sequences**. Sequences of sgRNA
645 sequences are noted with the PAM sequence in parentheses. Primer sequences are
646 listed for each locus.

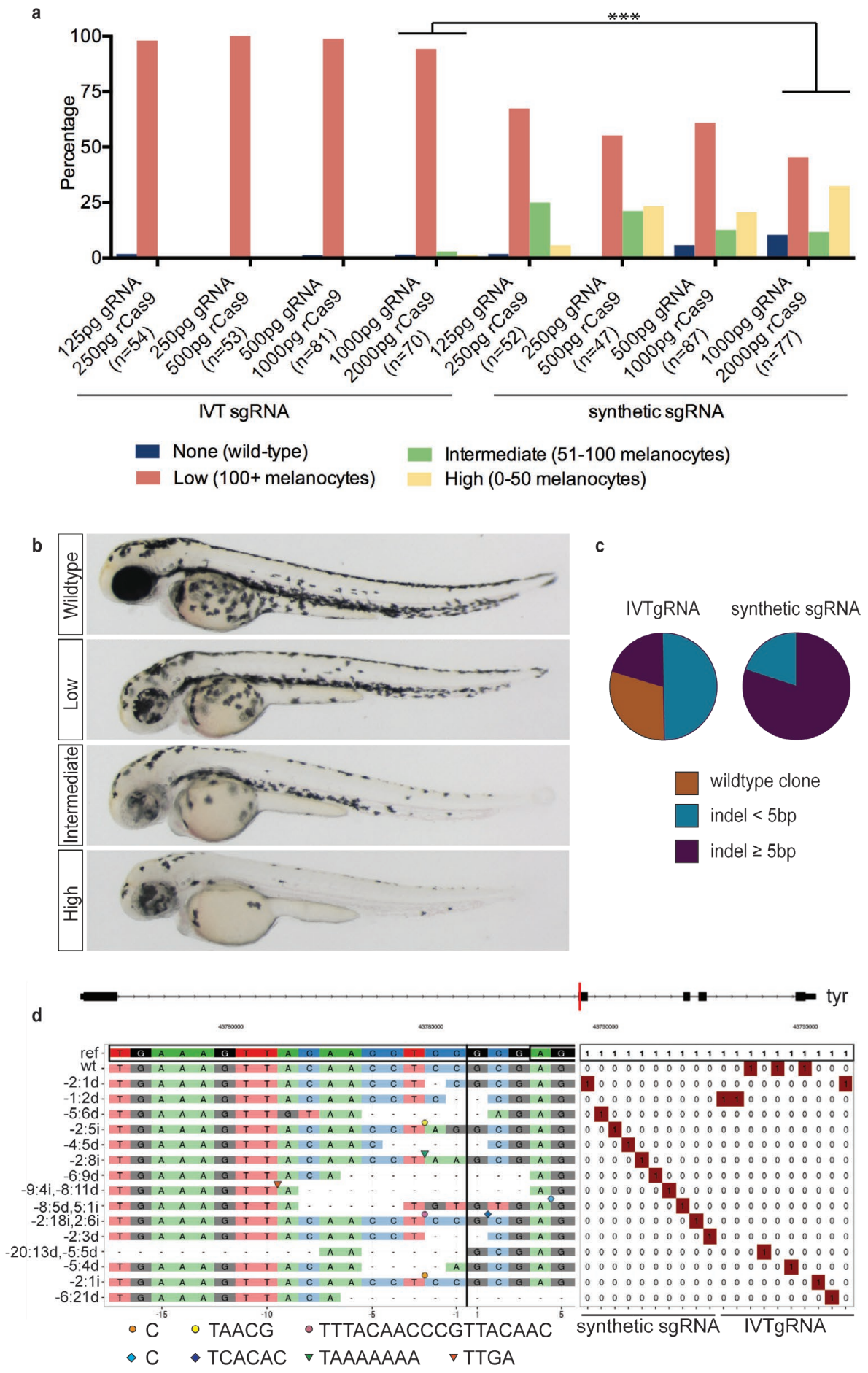
a
***
Percentage
100
75
50
25
0
125pg gRNA 250pg rCas9 (n=54)
250pg gRNA 500pg rCas9 (n=53)
500pg gRNA 1000pg rCas9 (n=81)
1000pg gRNA 2000pg rCas9 (n=70)
125pg gRNA 250pg rCas9 (n=52)
250pg gRNA 500pg rCas9 (n=47)
500pg gRNA 1000pg rCas9 (n=87)
1000pg gRNA 2000pg rCas9 (n=77)
IVT sgRNA
synthetic sgRNA
None (wild-type)
Low (100+ melanocytes)
Intermediate (51-100 melanocytes)
High (0-50 melanocytes)
b
Wildtype
Low
Intermediate
High
c
IVTgRNA
synthetic sgRNA
wildtype clone
indel < 5bp
indel ≥ 5bp
d
tyr
ref
wt
-2:1d
-1:2d
-5:6d
-2:5i
-4:5d
-2:8i
-6:9d
-9:4i,-8:11d
-8:5d,5:1i
-2:18i,2:6i
-2:3d
-20:13d,-5:5d
-5:4d
-2:1i
-6:21d
C
TAACG
TTTACAACCCGTTACAAC
C
TCACAC
TAAAAAAA
TTGA
synthetic sgRNA
IVTgRNA

Figure 1

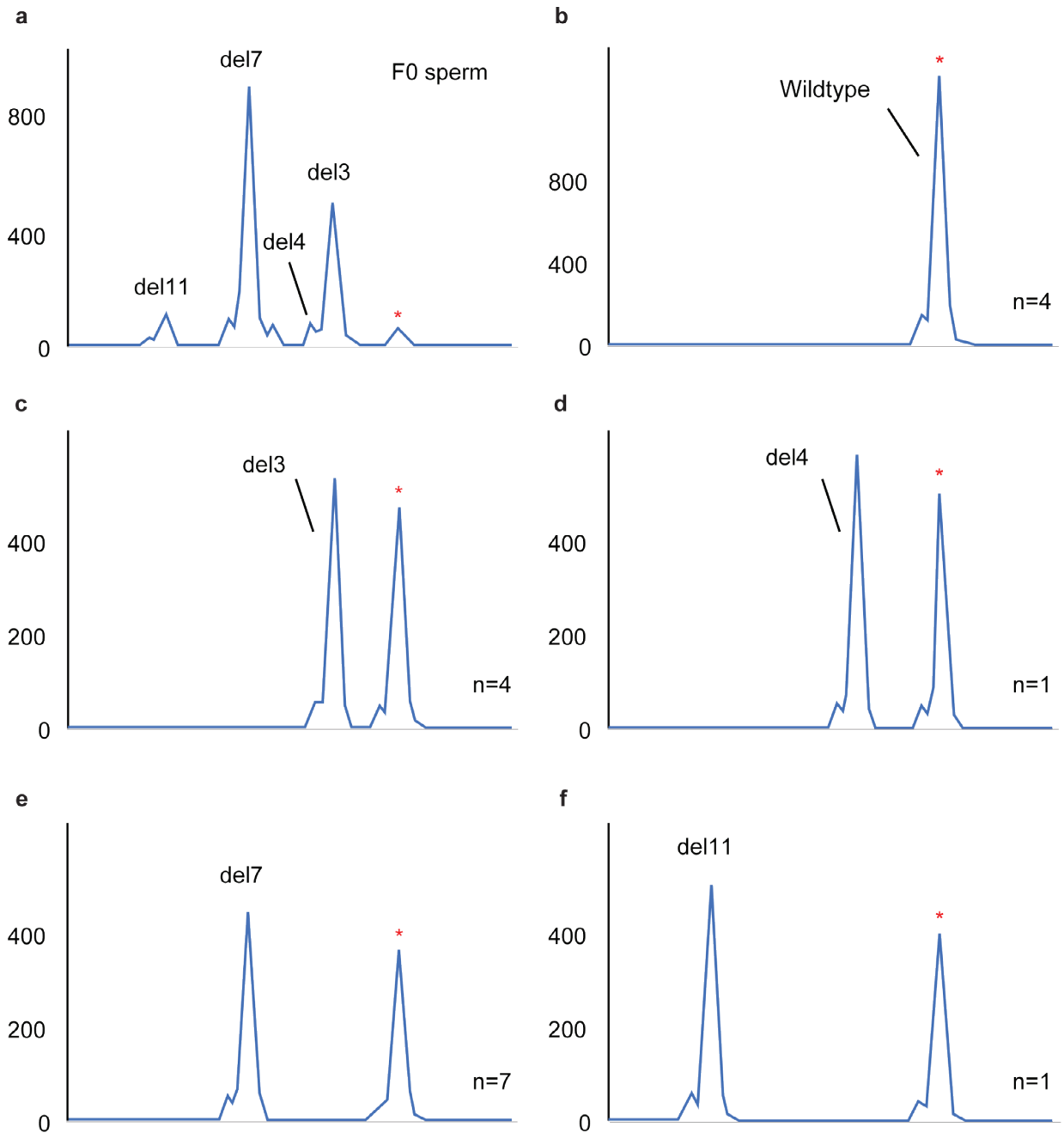
a
del7
F0 sperm
800
400
del3
del4
del11
*
0
b
Wildtype
*
800
400
n=4
0
c
del3
*
400
200
n=4
0
d
del4
*
400
200
n=1
0
e
del7
*
400
200
n=7
0
f
del11
*
400
200
n=1
0

Figure 2

a

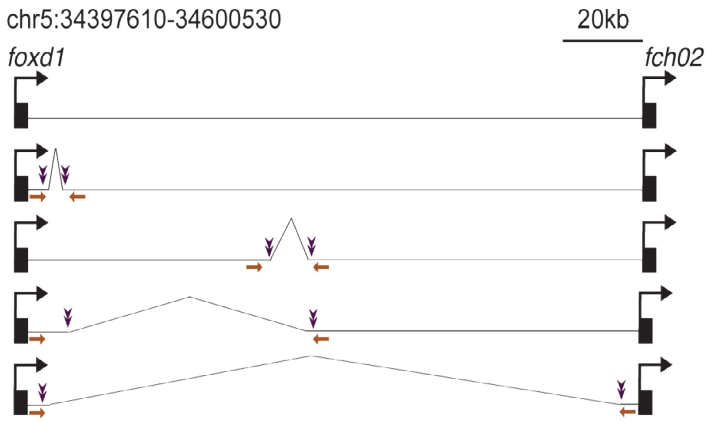

b

sgRNAs	Predicted deletion size	Observed deletion frequency
sgRNA1+2	0.45kb	5/10 (50%)
sgRNA3+4	4.3kb	7/24 (29%)
sgRNA2+4	52kb	3/8 (38%)
sgRNA1+5	124kb	2/23 (9%)

c

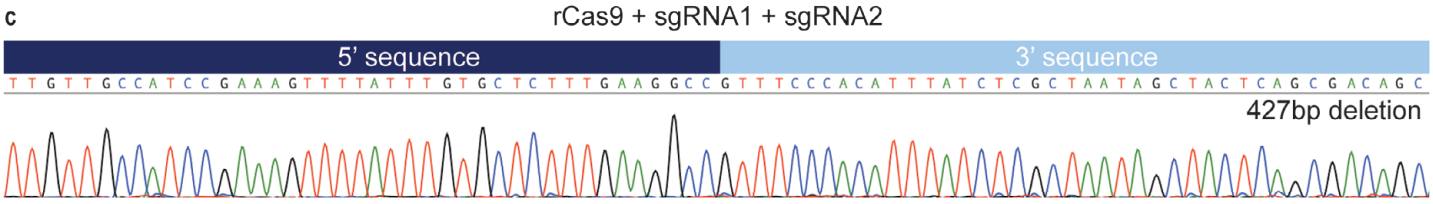

d

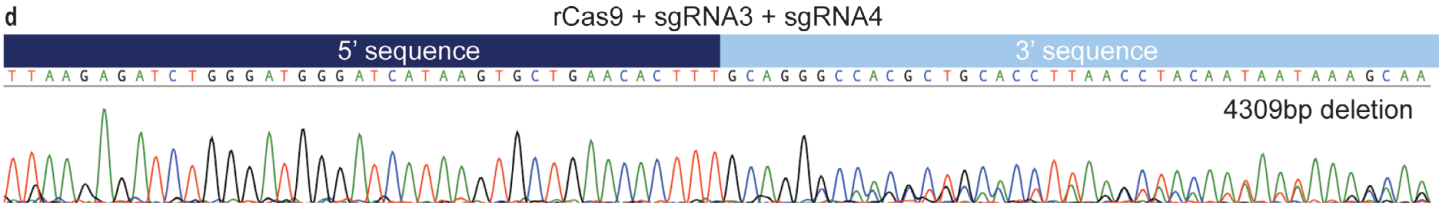

e

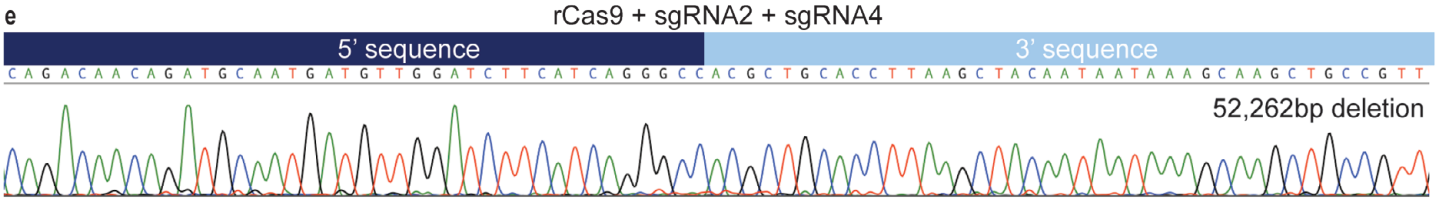

f

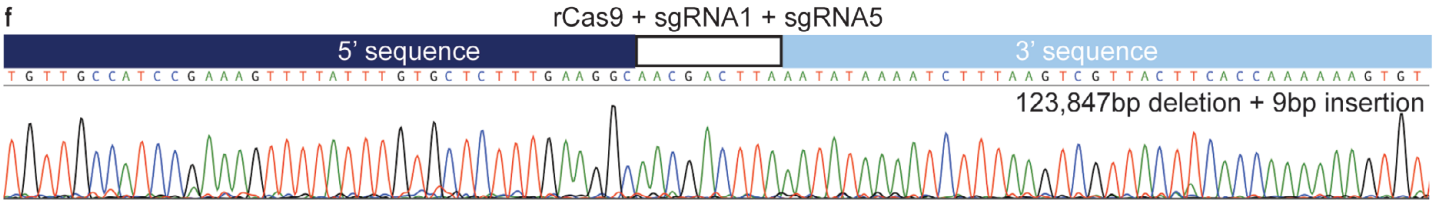

Figure 3

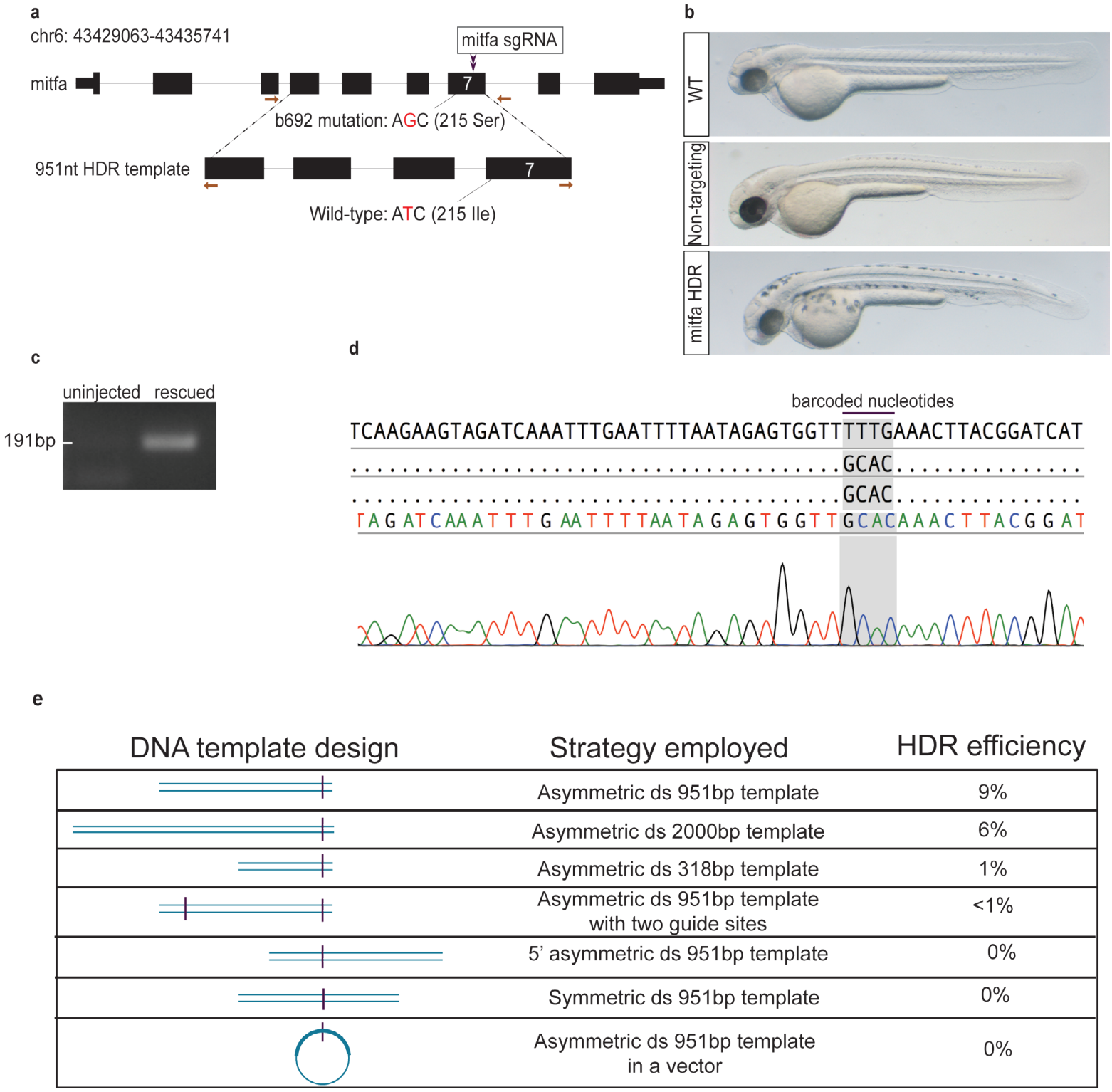
a
chr6: 43429063-43435741
mitfa sgRNA
mitfa
7
b692 mutation: AGC (215 Ser)
951nt HDR template
7
Wild-type: ATC (215 Ile)
b
WT
Non-targeting
mitfa HDR
c
uninjected
rescued
191bp
d
barcoded nucleotides
TCAAGAAGTAGATCAAATTTGAATTTTAATAGAGTGGTTTTTGAAACTTACGGATCAT
GCAC
GCAC
TAGATCAAATTTGAATTTTAATAGAGTGGTTGCACAAACTTACGGAT
e
DNA template design
Strategy employed
HDR efficiency
Asymmetric ds 951bp template
9%
Asymmetric ds 2000bp template
6%
Asymmetric ds 318bp template
1%
Asymmetric ds 951bp template with two guide sites
<1%
5' asymmetric ds 951bp template
0%
Symmetric ds 951bp template
0%
Asymmetric ds 951bp template in a vector
0%

Figure 4

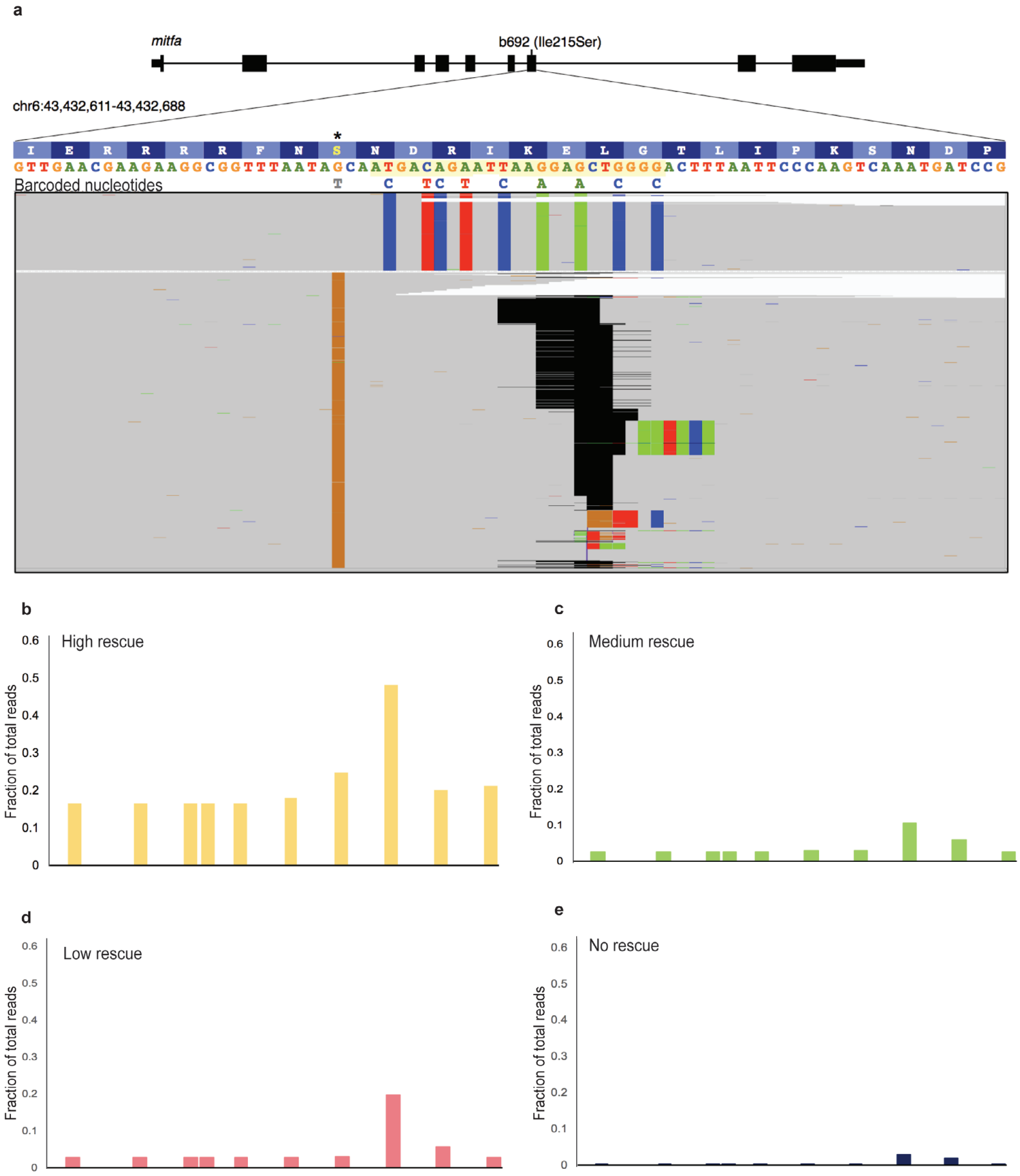
a
mitfa
b692 (Ile215Ser)
chr6:43,432,611-43,432,688
I E R R R R F N S N D R I K E L G T L I P K S N D P
GTTGAACGAAGAAGGCGGTTTAATAGCAATGACAGAATTAAGGAGCTGGGGACTTTAATTCCCAAGTCAAATGATCCG
Barcoded nucleotides
T C TC T C A A C C
b
High rescue
Fraction of total reads
0.6
0.5
0.4
0.3
0.2
0.1
0
c
Medium rescue
Fraction of total reads
d
Low rescue
Fraction of total reads
e
No rescue
Fraction of total reads

Figure 5

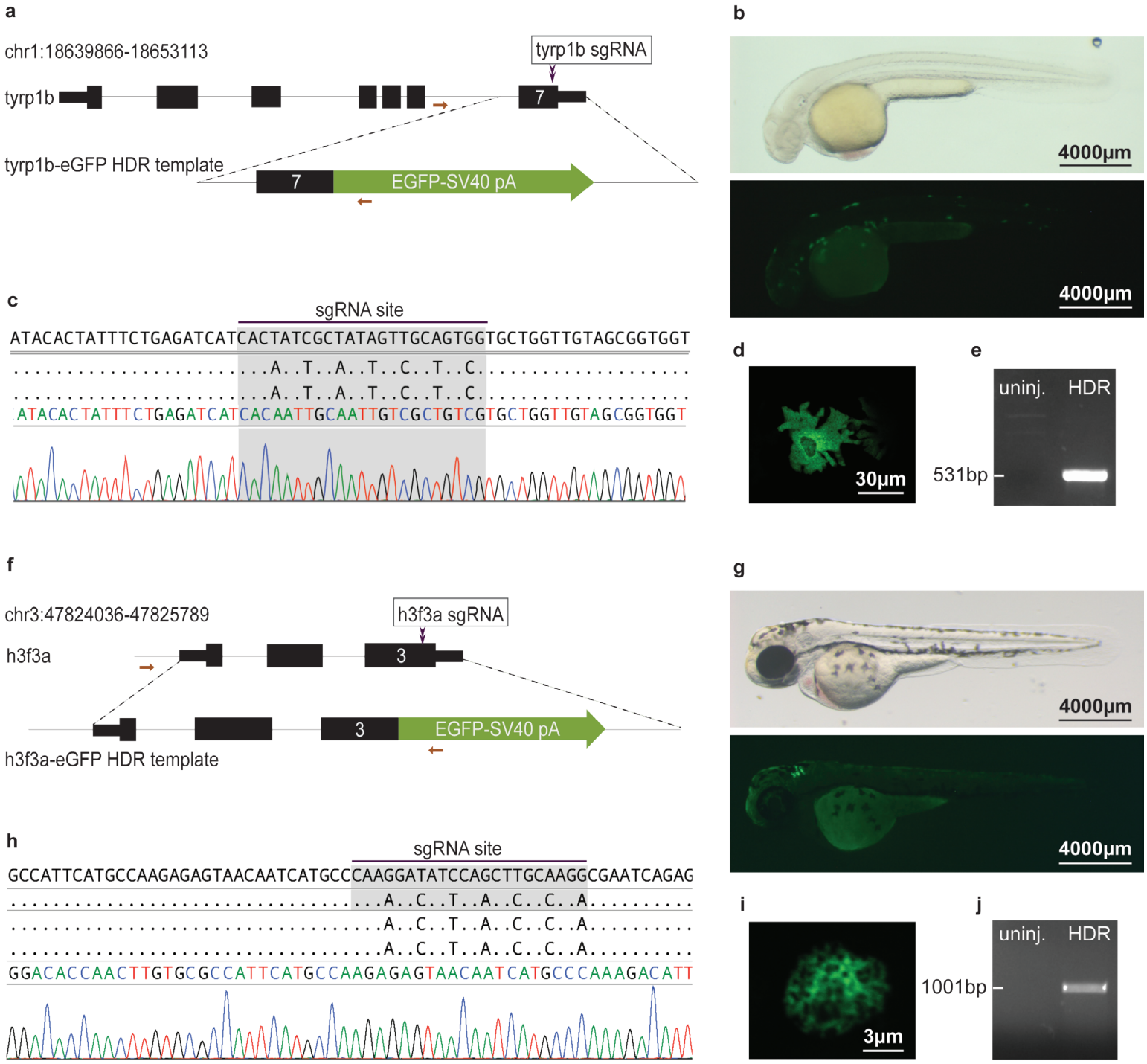
a
chr1:18639866-18653113
tyrp1b sgRNA
tyrp1b
7
tyrp1b-eGFP HDR template
7
EGFP-SV40 pA
b
4000μm
4000μm
c
sgRNA site
ATACACTATTTCTGAGATCATCACTATCGCTATAGTTGCAGTGGTGCTGGTTGTAGCGGTGGT
ATACACTATTTCTGAGATCATCACAATTGCAATTGTCGCTGTCGTGCTGGTTGTAGCGGTGGT
d
30μm
e
uninj.
HDR
531bp
f
chr3:47824036-47825789
h3f3a sgRNA
h3f3a
3
3
EGFP-SV40 pA
h3f3a-eGFP HDR template
g
4000μm
4000μm
h
sgRNA site
GCCATTCATGCCAAGAGAGTAACAATCATGCCCAAGGATATCCAGCTTGCAAGGCGAATCAGAG
GGACACCAACTTGTGCGCCATTCATGCCAAGAGAGTAACAATCATGCCCAAAGACATT
i
3μm
j
uninj.
HDR
1001bp

Figure 6

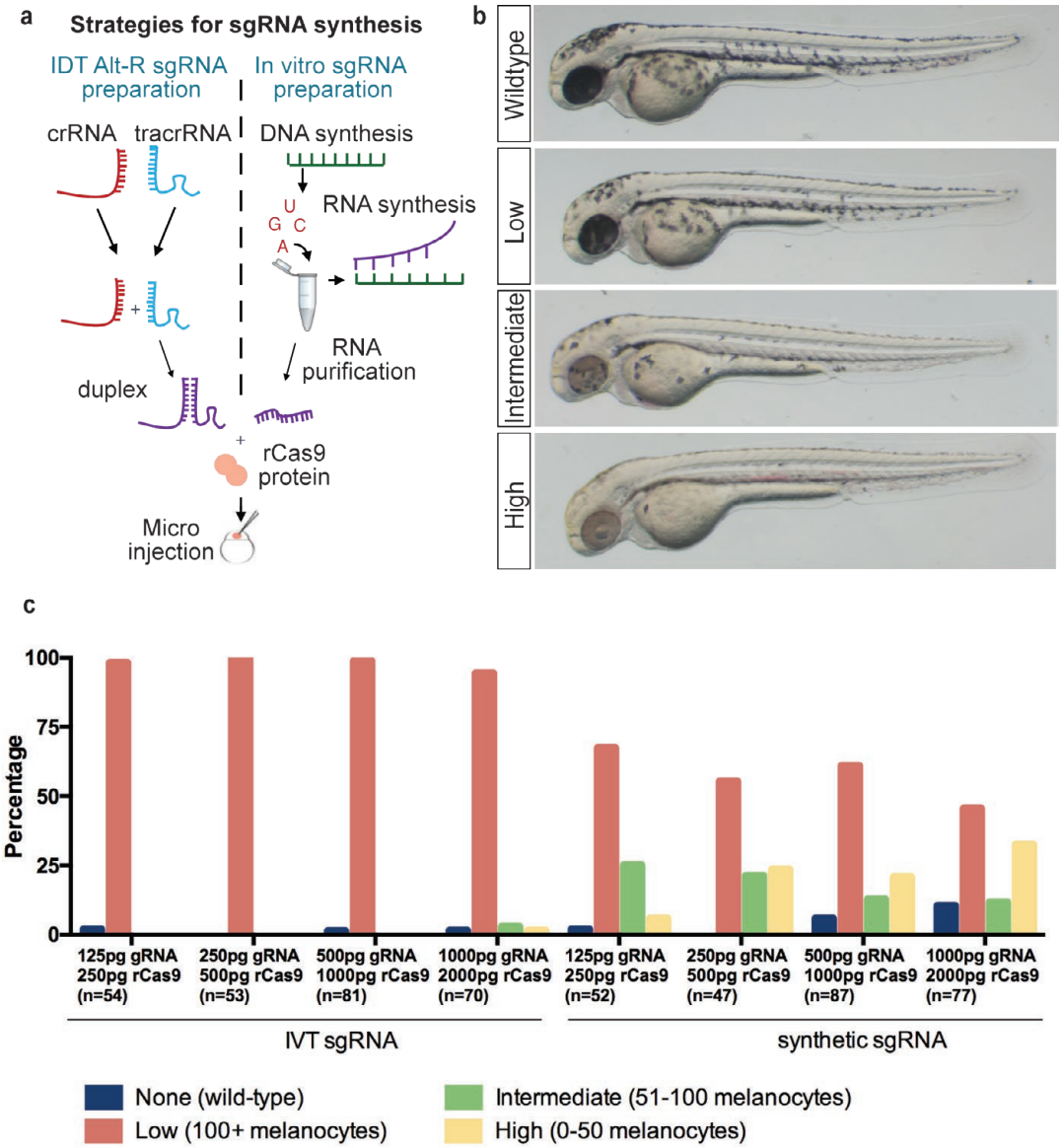

Supplementary Figure 1

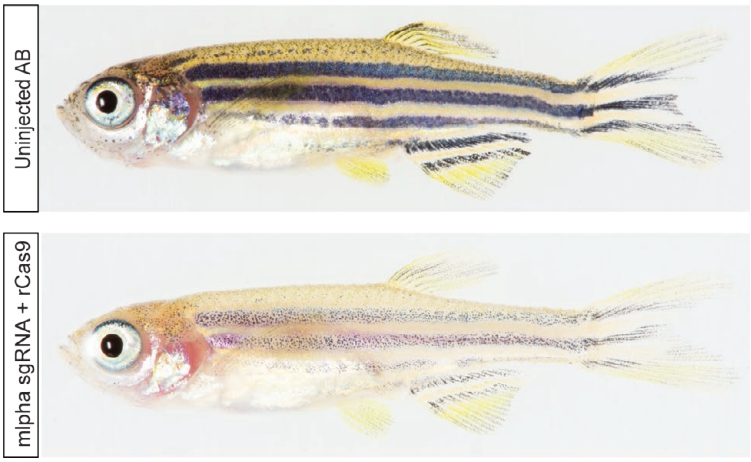

Supplementary Figure 2

	F0 Sperm	F1 Progeny
del11	7.4%	5.9%
del7	58.9%	41.2%
del4	<5%	5.9%
del3	33.7%	23.5%
WT	<5%	23.5%
Total	100.0%	100.0%

Supplementary Figure 3

a

rCas9 + sgRNA 1 + sgRNA 2

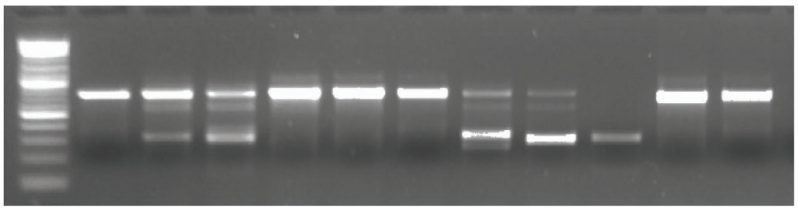

b

427bp deletion + 0bp insertion

c

rCas9 + sgRNA 3 + sgRNA 4

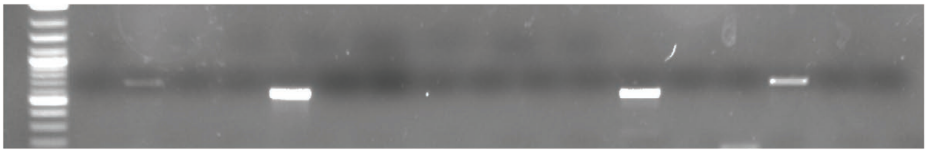

d

4297bp deletion + 21bp insertion
4298bp deletion + 15bp insertion
4302bp deletion + 34bp insertion
4316bp deletion + 0bp insertion
4451bp deletion + 40bp insertion

e

rCas9 + sgRNA 2 + sgRNA 3

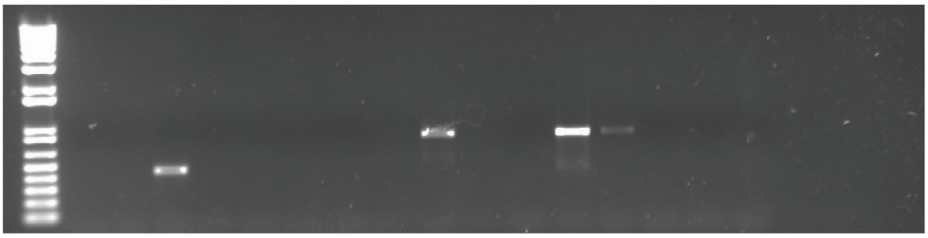

f

52262 bp deletion + 0bp insertion
52266 bp deletion + 12bp insertion

g

rCas9 + sgRNA 1 + sgRNA 5

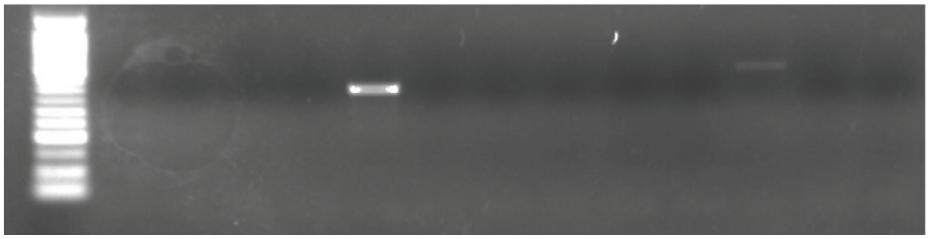

h

123847bp deletion + 9bp insertion

Supplementary Figure 4

a

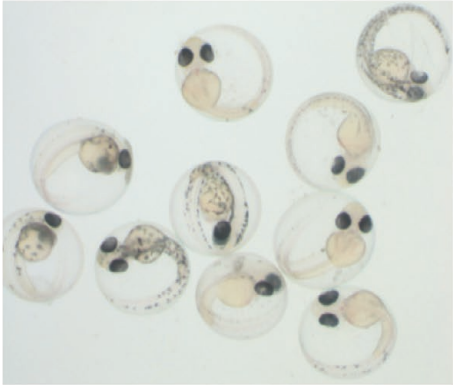

b

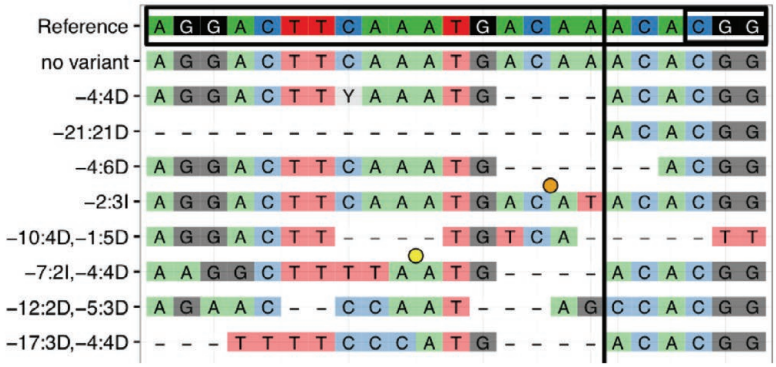

c

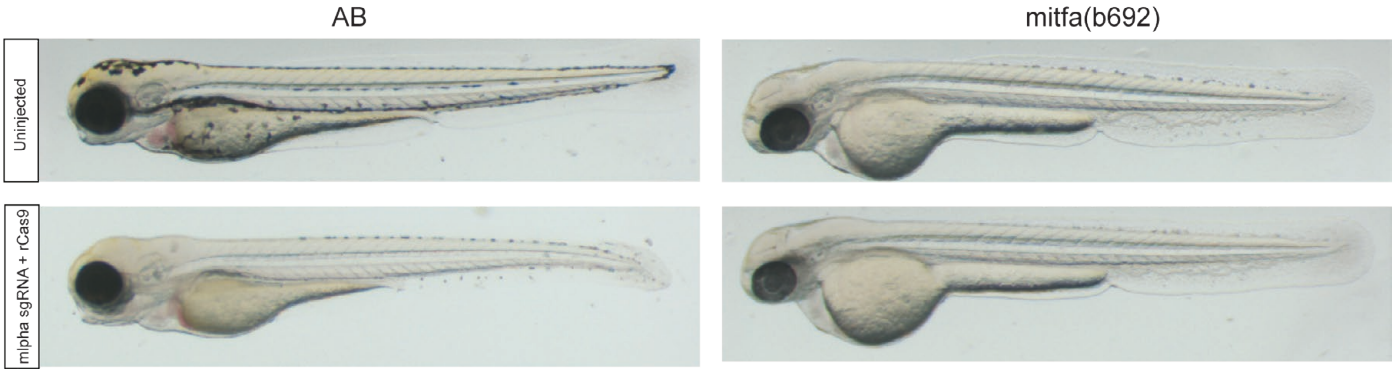

Supplementary Figure 5

DNA template design	Strategy employed	HDR efficiency
	Symmetric ds 76bp template	0%
	Symmetric ds 200bp template	0%
	Asymmetric ds 951bp template with nickase-compatible guide sites	0%
	Asymmetric ds 951bp template with nonhomologous flanking guide sites	0%
	Symmetric ds 2000bp template	0%
	Symmetric ds 1214bp template with homologous flanking guide sites	0%
	Symmetric ds 896bp template with two guide sites	0%
	Asymmetric ds 951bp template with flanking IScel restriction enzyme sites	0%
	Symmetric ss 896nt template with two guide sites	0%
	Symmetric ss 200bp template	0%

Supplementary Figure 6

gRNA name	gRNA sequence
tyr	TGAAAGTTACAACCTCCGCG(AGG)
slc24a5	GGTCTCTCGCAGGATGTTGC(TGG)
mitfa(w2)	AGGACTTCAAATGACAAACA(CGG)
b692	ATGACAGAATTAAGGAGCTG(GGG)
tyrp1b	CACTATCGCTATAGTTGCAG(TGG)
mlpha	AATGACCTCCCACACATGCT(TGG)
h3f3a	CAAGGATATCCAGCTTGCA(AGG)
non-targeting	TGCTGATGTCTTGGTTGAAT(TGG)
deletion_1	TGTGCTCTTTGAAGGCCATG(AGG)
deletion_2	TGTGGGAAACGGCATATATG(AGG)
deletion_3	AATCACCGAGAAAATTGGAG(AGG)
deletion_4	CAGGCAGGATCAAAGAAGGC(AGG)
deletion_5	AATAGCTCATAAAGACGGTG(AGG)
slc6a15	GACTCCATCTCAGAGGGTGG(AGG)

Primer Name	Primer sequences
tyr_guide_validation (F)	AATGTCGTTCACTCTGCTGTTG
tyr_guide_validation (R)	GTGACCGTGCTGTTGTACCTT
mitfa_w2_guide_validation (F)	GTGGATTGAGGTTCCCTTCA
mitfa_w2_guide_validation (R)	CGGATAATTCCCTTTTGACG
mitfa_HDR_detection (F)	GCTACAGTGATGACATTCTTGG
mitfa_HDR_detection (R)	GCATGATTGCTGTACATATCAAGCAAA
mitfa_next_gen (F)	GCAGTTATTAATGATAATGTCTCG
mitfa_next_gen (F)	GGACTTAAGTAAATCAAGAAGTAGATC
downstream_foxd1_deletion_1 (F)	TCACTGAGGCCTCTGACAGA
downstream_foxd1_deletion_2 (R)	TACTCCTTTGGACAGGGCCA
downstream_foxd1_deletion_3 (F)	CTCTGTGGTCTATTTCTCTCC
downstream_foxd1_deletion_4 (R)	CAGAAGGTGAAGCAGCCTCA
downstream_foxd1_deletion_5 (R)	ACCACGTCTTCAAGGGCTTC

Supplementary Figure 7